

Three different configurations of d^{10} complexes based on benzoxazole pyridyl ligand: Synthesis, structures and properties

Shanshan Mao, Han Zhang, Kesheng Shen, Yuling Xu, Xinkui Shi, Huilu Wu*

School of Chemical and Biological Engineering, Lanzhou Jiaotong University, Lanzhou, Gansu 730070, PR China

ARTICLE INFO

Article history:

Received 3 May 2017

Accepted 24 June 2017

Available online 4 July 2017

Keywords:

Transition metal complexes

Synthesis

Crystal structure

Fluorescence

Electrochemical studies

ABSTRACT

Three different coordination complexes containing 2-(3'-pyridyl)-benzoxazole (3-PBO) and 2-(4'-pyridyl)-benzoxazole (4-PBO) ligands, namely $[Cd(3\text{-PBO})_2(NO_3)_2(H_2O)_2]CH_3CN$ (**1**), $[Zn(4\text{-PBO})_2(NO_3)_2]$ (**2**) $[Ag(4\text{-PBO})_2Pic]_n$ ($Pic = Picric acid$) (**3**) have been synthesized and characterized. Single crystal X-ray structure analysis reveals that complex **1** is distorted seven-coordinated pentagonal-bipyramidal geometry, and complex **2** is a twisted six-coordinate octahedral structure, while complex **3** is a four-coordinated one-dimensional linear coordination polymer. A wide range of hydrogen bonding (of the O-H \cdots O and O-H \cdots N types) and π - π stacking interactions are also present in the crystal structure. These arrangements lead to the formation of three supramolecular structures. By careful inspection of the structures of **1** and **2**, the ion radius of metal centers adopting various coordination modes is a crucial factor for the formation of the different structures. Cyclic voltammograms of **3** indicate a quasi-reversible Ag^+/Ag couple. Moreover, the fluorescence properties of the ligands and complexes **1**–**3** were studied in solid state. Strong photoluminescence is observed in complexes **1** and **2** at room temperature and the complexes may be good candidates for potential luminescence materials.

© 2017 Elsevier Ltd. All rights reserved.

1. Introduction

Over the past decade, the rational design and assembly of metal–organic frameworks have extensive interest in coordination and supramolecular chemistry because of its intriguing structure and potential applications in functional materials [1–3]. However, the ability to predict and control supramolecular assembly is still a long-term challenge due to the fact that the self-assembly process is frequently influenced by various factors, including in being of the metal ions and the predesigned organic ligands as well as other factors such as medium, template, temperature and counterion [4,5]. With regard to the efforts to pursue the supramolecular framework synthesis strategy, some noncovalent forces, such as π – π stacking interactions and hydrogen bonding interactions, also intensively impact the supramolecular topology and dimensionality [6,7]. The ligands containing 2-substituted benzimidazoles/benzoxazoles have a wide range of interest for their antiviral activity [8], luminescent properties [9,10], multifunctional coordination patterns, and the potential to form supramolecular aggregates through π – π stacking interactions [10,11].

Complexes of d^{10} metal ions such as zinc(II), cadmium(II), and silver(I) have recently drawn global attention due to these metals

playing important roles in many newer functional materials [12–14]. Zinc-containing compounds are particularly noticeable as luminescent materials for organic light-emitting diodes [15], and promote the various structures that can be used for sensory materials to detect alkaloids [16] and nitro aromatics [17]. Cd (II) is usually used in the field of optics such as fluorescent probes and nonlinear optical materials [18–21]. Ag(I) ions are more compatible with the electrical, photographic, imaging and pharmaceutical industries [22,23], the complexes of which exhibit different coordination geometries and luminescent properties [24].

In our previous work, we have investigated a series of V-shaped bis-benzimidazole ligands and their complexes [25]. However, little is known on the use of the title ligands. Hence, in this work, we wish to report the synthesis, structure, fluorescence studies, and electrochemical properties of three d^{10} metal complexes containing benzoxazole pyridyl ligands.

2. Experimental details

2.1. Materials and methods

All chemicals and solvents were reagent grade and were used without further purification. The C, H and N elemental analyses were performed using a Carlo Erba 1106 elemental analyzer. The

* Corresponding author.

E-mail address: wuhuilu@163.com (H. Wu).

thermal analysis of the complexes **1–3** were carried out under nitrogen atmosphere with a heating rate of 10 °C/min on METTLER TOLEDO TGA1. The IR spectra were recorded in the 4000–400 cm⁻¹ region with a Nicolet FT-VERTEX 70 spectrometer using KBr pellets. Electronic spectra were taken on a Lab-Tech UV Bluestar spectrophotometer. Absorbance was measured with the Spectrumlab 722sp spectrophotometer at room temperature. ¹H NMR spectra were recorded on a Varian VR300-MHz spectrometer with TMS as an internal standard. Fluorescence measurements were performed on a 970-CRT spectrofluorophotometer. Electrochemical measurements were performed on a LK2005A electrochemical analyser under nitrogen at 283 K. A glassy carbon working electrode, a platinum-wire auxiliary electrode and a Ag/AgCl reference electrode ($[Cl^-] = 1.0 \text{ mol/L}$) were used in the three-electrode measurements. The electroactive component was at $1.0 \times 10^{-3} \text{ mol}\cdot\text{dm}^{-3}$ concentration with tetrabutylammonium perchlorate (TBAP) (0.1 mol·dm⁻³) used as the supporting electrolyte in DMF. Ag(Pic) is obtained by reacting silver carbonate with picric acid.

2.2. Synthesis of the ligands and complexes **1–3**

The ligands 3-PBO and 4-PBO (Scheme 1) were synthesized according to the reported method [26].

Three complexes were prepared using a similar procedure. Complex **1** was prepared by the following reaction. A solution of 3-PBO (0.0392 g, 0.2 mmol) in 3 mL of dichloromethane was very carefully placed on the bottom of the tube. 1 mL of dichloromethane as the buffer was slowly layered onto the ligand solution. A clear solution of Cd(NO₃)₂·4H₂O (0.0308 g, 0.1 mmol) in 3 mL of acetonitrile was then very carefully layered on the top of the buffer solution. After 1 week, colorless block crystals of **1** were collected by filtration and dried in vacuo. The synthesis of complex **2** is similar to **1** except for using 4-PBO (0.0392 g, 0.2 mmol) and Zn(NO₃)₂·6H₂O (0.0291 g, 0.1 mmol) instead of 3-PBO and Cd(NO₃)₂·4H₂O. Complex **3** was synthesized similar to **2**, but using Ag(Pic) (0.0336 g, 0.1 mmol) instead of Zn(NO₃)₂·6H₂O.

[Cd(3-PBO)₂(H₂O)₂]CH₃CN (**1**), Yield: 52%. Elemental analysis for C₂₆H₂₃CdN₇O₁₀: calculated (%): C, 44.24; H, 3.28; N, 13.89. Found (%): C, 44.33; H, 3.41; N, 13.76. Selected-IR (KBr;

cm⁻¹): 1617 ν(C=C), 1401 ν(C=N), 1300 ν(NO₃⁻), 1041 ν(NO₃⁻), 1240 ν(C—O). UV-Vis (in DMF), λ_{\max} (nm): 303.

[Zn(4-PBO)₂(NO₃)₂] (**2**), Yield: 54%. Elemental analysis for C₂₄H₁₆N₆O₈Zn: calculated (%): C, 49.55; H, 2.77; N, 14.44. Found (%): C, 49.45; H, 2.65; N, 14.31. Selected-IR (KBr; cm⁻¹): 1628 ν(C=C), 1413 ν(C=N), 1346 ν(NO₃⁻), 1032 ν(NO₃⁻), 1216 ν(C—O). UV-Vis (in DMF), λ_{\max} (nm): 302.

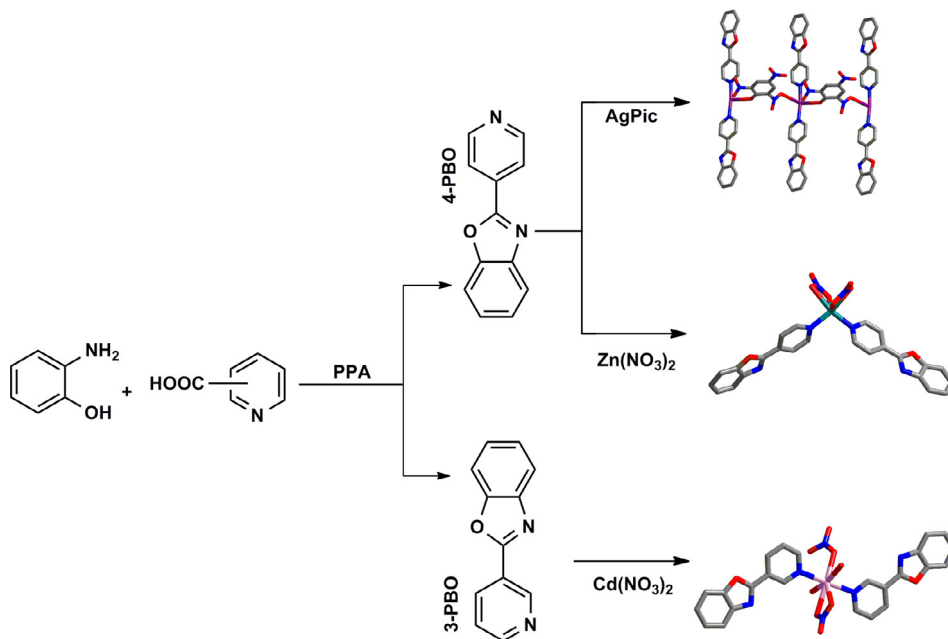
[Ag(4-PBO)₂Pic]_n (**3**), Yield: 51%. Elemental analysis for C₃₀H₁₈AgN₇O₉: calculated (%): C, 49.47; H, 2.49; N, 13.46. Found (%): C, 49.33; H, 2.44; N, 13.55. Selected-IR (KBr; cm⁻¹): 1589 ν(C=C), 1395 ν(C=N), 1336 ν(Ar—NO₂), 1232 ν(C—O). UV-Vis (in DMF), λ_{\max} (nm): 303 and 380.

2.3. X-ray crystallography

Suitable single crystals of complexes **1–3** were mounted on a glass fiber, and the intensity data were collected on a Bruker APEX II area detector with graphite-monochromated Mo Ka radiation ($\lambda = 0.71073 \text{ \AA}$) at 296(2) K. Data reduction and cell refinement were performed using the SMART and SAINT programs [27]. The absorption corrections are carried out by the empirical method. The structure was solved by direct methods and refined by full-matrix least squares against F² of data using SHELXTL software. [28] All H atoms were found in different electron maps and were subsequently refined in a riding-model approximation with C-H distances ranging from 0.95 to 0.99 Å. Information concerning the crystallographic data collection and structural refinements is summarized in Table 1. The relevant bond lengths and angles are listed in Table 2.

3. Results and discussion

Synthetic routes towards ligands and d¹⁰ metal complexes are exhibited in Scheme 1. The three complexes were obtained by the reaction of Cd(NO₃)₂, Zn(NO₃)₂ and Ag(Pic) with two ligands, namely, 3-PBO and 4-PBO, in acetonitrile and dichloromethane. They are soluble in polar aprotic solvents such as DMF, DMSO and MeCN, slightly soluble in ethanol, methanol, ethyl acetate, acetone and chloroform, and insoluble in Et₂O and petroleum ether.



Scheme 1. Synthesis of ligands and complexes **1–3**.

Table 1Crystal and structure refinement data for complexes **1–3**.

Complex	1	2	3
Empirical formula	C ₂₆ H ₂₃ CdN ₇ O ₁₀	C ₂₄ H ₁₆ N ₆ O ₈ Zn	C ₃₀ H ₁₈ AgN ₇ O ₉
Molecular weight (gm ⁻¹)	705.91	581.82	728.38
Crystal system	triclinic	monoclinic	triclinic
Space group	P $\bar{1}$	C $2/c$	P $\bar{1}$
<i>Unit cell dimensions</i>			
<i>a</i> (Å)	7.2224(11)	11.6344(18)	8.3903(9)
<i>b</i> (Å)	13.4212(18)	8.3896(12)	10.5988(10)
<i>c</i> (Å)	15.367(2)	24.534(4)	17.1211(16)
α (°)	98.219(2)	90	101.068(2)
β (°)	103.490(2)	94.987(2)	100.4900(10)
γ (°)	102.207(2)	90	99.197(2)
<i>V</i> (Å ³)	1386.5(3)	2385.6(6)	1439.0(2)
<i>Z</i>	2	4	2
<i>D</i> _{calc} (g cm ⁻³)	1.691	1.620	1.681
Absorption coefficient (mm ⁻¹)	0.859	1.094	0.771
<i>F</i> (000)	712	1184	732
Crystal size (mm)	0.43 × 0.34 × 0.30	0.46 × 0.33 × 0.31	0.47 × 0.38 × 0.31
θ range for data collection (°)	1.39–25.50	3.00–25.48	1.24–25.50
Reflections collected	7289	6122	7619
Independent reflections	5116 [<i>R</i> _{int} = 0.0159]	2221 [<i>R</i> _{int} = 0.0203]	5299 [<i>R</i> _{int} = 0.0216]
Index ranges	$-8 \leq h \leq 6, -11 \leq k \leq 16, -18 \leq l \leq 18$	$-13 \leq h \leq 14, -10 \leq k \leq 7, -28 \leq l \leq 29$	$-10 \leq h \leq 10, -12 \leq k \leq 12, -19 \leq l \leq 20$
Refinement method	Full-matrix least-squares on <i>F</i> ²	Full-matrix least-squares on <i>F</i> ²	Full-matrix least-squares on <i>F</i> ²
Data/restraints/parameters	5116/2/414	2221/1/177	5299/0/425
Goodness-of-fit on <i>F</i> ²	1.119	1.091	1.056
Finial <i>R</i> ₁ and <i>wR</i> ₂ [<i>I</i> > 2σ(<i>I</i>)]	<i>R</i> ₁ = 0.0316, <i>wR</i> ₂ = 0.0989	<i>R</i> ₁ = 0.0380, <i>wR</i> ₂ = 0.1087	<i>R</i> ₁ = 0.0351, <i>wR</i> ₂ = 0.0931
<i>R</i> indices (all data)	<i>R</i> ₁ = 0.0356, <i>wR</i> ₂ = 0.1097	<i>R</i> ₁ = 0.0407, <i>wR</i> ₂ = 0.1110	<i>R</i> ₁ = 0.0429, <i>wR</i> ₂ = 0.0996
Largest diff. peak and hole (e Å ⁻³)	0.695 and -0.663	0.427 and -0.371	0.353 and -0.639

Table 2Selected bond distances (Å) and angles (°) for complexes **1–3**.

Complex 1			
Cd(1)–N(2)	2.314(3)	Cd(1)–N(4)	2.308(3)
Cd(1)–O(10)	2.332(3)	Cd(1)–O(9)	2.334(3)
Cd(1)–O(5)	2.401(3)	Cd(1)–O(6)#1	2.530(3)
Cd(1)–O(6)	2.530(3)	Cd(1)–O(8)	2.579(3)
N(4)–Cd(1)–N(2)	179.36(8)	N(4)–Cd(1)–O(10)	87.23(13)
N(2)–Cd(1)–O(10)	93.06(13)	N(4)–Cd(1)–O(9)	93.56(11)
N(2)–Cd(1)–O(9)	86.00(11)	O(10)–Cd(1)–O(9)	164.67(12)
N(4)–Cd(1)–O(5)	86.64(10)	N(2)–Cd(1)–O(5)	92.77(10)
O(10)–Cd(1)–O(5)	93.57(12)	O(9)–Cd(1)–O(5)	71.21(11)
N(4)–Cd(1)–O(6)#1	89.82(10)	N(2)–Cd(1)–O(6)#1	90.81(9)
O(10)–Cd(1)–O(6)#1	73.23(11)	O(9)–Cd(1)–O(6)#1	122.06(10)
O(5)–Cd(1)–O(6)#1	166.50(10)	N(4)–Cd(1)–O(6)	89.82(10)
Complex 2			
Zn(1)–N(2)	2.037(2)	Zn(1)–N(2)#2	2.037(2)
Zn(1)–O(3)#2	2.056(2)	Zn(1)–O(3)	2.056(2)
Zn(1)–O(4)#2	2.380(2)	Zn(1)–O(4)	2.380(2)
N(2)–Zn(1)–N(2)#2	103.54(12)	N(2)–Zn(1)–O(3)#2	103.01(8)
N(2)–Zn(1)–N(2)	105.63(9)	N(2)–Zn(1)–O(3)	105.63(9)
N(2)–Zn(1)–O(3)	103.01(8)	O(3)–Zn(1)–O(3)	132.90(12)
N(2)–Zn(1)–O(4)#2	158.73(8)	N(2)–Zn(1)–O(4)#2	90.18(9)
Complex 3			
Ag(1)–N(4)	2.179(3)	Ag(1)–N(2)	2.189(3)
Ag(1)–O(9)	2.646(2)	Ag(1)–O(4)	2.808(6)
N(4)–Ag(1)–N(2)	173.15(9)	N(4)–Ag(1)–O(9)	89.64(9)
N(2)–Ag(1)–O(9)	95.09(9)	O(4)–Ag(1)–O(9)	125.39(6)

Symmetry transformations used to generate equivalent atoms: #1 *x,y,z*, #2 *-x+1, y, -z+1/2*.

3.1. X-Ray structure determination of complexes

The structures of **1–3** were confirmed by X-ray diffraction. The crystal structures are shown in Figs. 1, 3 and 5(a), respectively.

Complex **1** crystallizes in the triclinic space group *P* $\bar{1}$, and its ORTEP structure along with the atomic numbering scheme is shown in Fig. 1. According to the determined molecular structure, complex **1** consists of one neutral molecule, [Cd(3-PBO)₂(NO₃)₂(H₂O)₂] and one uncoordinated acetonitrile molecule. The central

cadmium atom in complex **1** is a seven-coordinated cadmium complex and has a distorted pentagonal-bipyramidal geometry (the common coordination geometry for seven-coordinated metal (II) complexes) [29]. As shown in Fig. 1, the equatorial sites are occupied by the five oxygen atoms, namely, two oxygen atoms of the water molecules (O9 and O10), two oxygen atoms of the chelating nitrate ligand (O6 and O8) and one oxygen atom of unidentate nitrate ion (O5). This arrangement leads to the formation of an approximately planar pentagon. The deviation from the perfect planar coordination mode (72°) is best illustrated by the O6–Cd1–O8 angle of 49.35(8)° due to the chelating nitrate ligand. 3-PBO ligands occupied the axial positions. The Cd–O bond distances of Cd(1)–O(10) = 2.332(3) Å, Cd(1)–O(9) = 2.334(3) Å, Cd(1)–O(5) = 2.401(3) Å, Cd(1)–O(6) = 2.530(3) Å, Cd(1)–O(8) = 2.579(3) Å and Cd–N bond lengths of Cd(1)–N(2) = 2.314(3) Å, Cd(1)–N(4) = 2.308(3) Å are close to those reported in the literatures [30–32].

The crystal packing of **1** is dominated by hydrogen bonding interactions between co-crystal water molecule and complex, and also π–π stacking interactions between oxazole rings defined by atoms C5/C6/O1/C7/N1 and C17/C18/O2/C19/N3 (Fig. 2). The structure shows the neighboring chains are connected by O–H···O, O–H···N and C–H···O hydrogen bonds (Table 3), in addition, the neighboring oxazole rings are stabilized by π–π stacking with centroid distances of 3.630 and 3.634 Å, thus generating an infinite 2-D layer (Fig. 2).

Complex **2** crystallizes in the monoclinic space group *C2/c*, and its ORTEP structure along with the atomic numbering scheme is shown in Fig. 3. The crystallographic data reveal that the molecular unit is centrosymmetric and is made up of equivalent halves. The symmetry transformations #1 *-x+1, y, -z+1/2* are used to generate equivalent atoms. All the equivalent bond lengths and angles around Zn(II) are equal (Table 2). The complex **2** comprises [Zn(4-PBO)₂] cation and two bidentate nitrate anions. The central zinc atom in complex **2** is six-coordinated structure consisting of N₂O₄ (two N2 atoms from two 4-PBO ligands, four oxygen atoms from two bidentate nitrate ions) as shown in Fig. 3. The coordination geometry of the zinc(II) may be best described as distorted octahe-

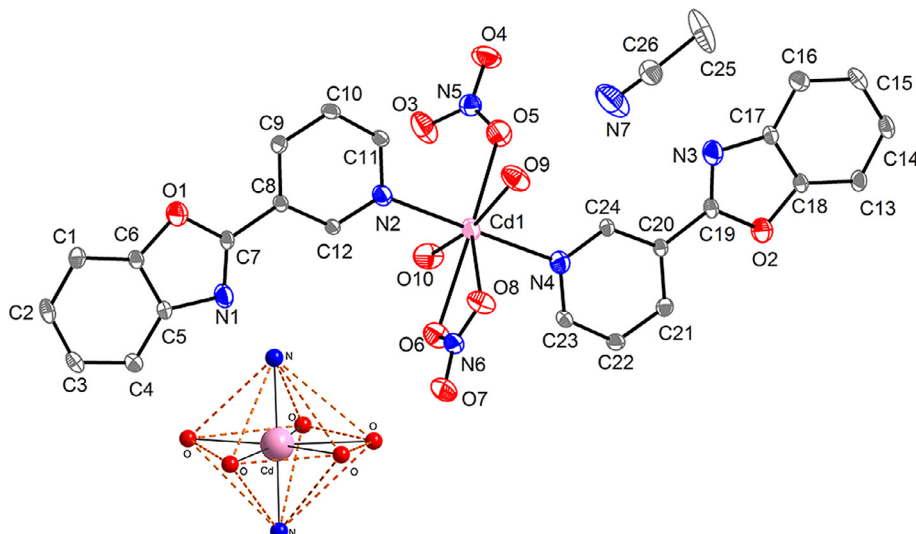


Fig. 1. Molecular structure and atom numberings of complex **1** showing displacement ellipsoids at the 30% probability level. Hydrogen atoms were omitted for clarity.

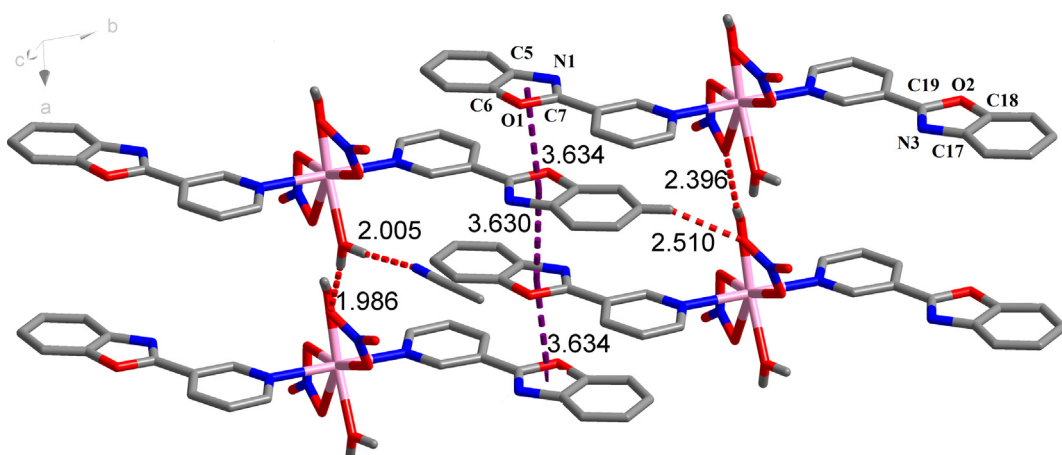


Fig. 2. 2-D layer generated by O-H...O, O-H...N and C-H...O hydrogen bonding and π - π stacking in complex **1**. Some atoms are omitted for clarity.

Table 3
Intermolecular hydrogen bonds for complex **1**.

D-H...A	d(D-H)	d(H...A)	d(D...A)	\angle (DHA)
C(14)-H(14)...O(3) _{#3}	0.93	2.51	3.395(5)	158.4
O(9)-H(20)...O(3) _{#4}	0.84(6)	1.98(6)	2.822(4)	175(5)
O(9)-H(19)...N(7) _{#1}	0.83(5)	2.00(5)	2.831(6)	175(5)
O(10)-H(18)...O(8) _{#5}	0.66(6)	2.39(6)	3.001(5)	156(7)

Symmetry transformations used to generate equivalent atoms: #1 x,y,z, #3 x + 1,y + 1,z, #4 x + 1,y,z, #5 x - 1,y,z.

dral with (O3A,O4,O3,N2A) providing the equatorial plane. The maximum deviation distance (O3) from the least squares plane calculated from the four coordination atom atoms is 0.190(5) Å, and the zinc atom is out of this plane by 0.410(7) Å.

The bond length between the zinc atom and the apical atoms (N2, O4A) are 2.037 and 2.380 Å, respectively. The bond angle of the two atoms (N2-Zn1-O4A) in axial positions is 158.726(87)°. Therefore, compared with the regular octahedral, the geometry around the Zn(II) is a relatively distorted octahedron [33–36]. Besides, in the crystal structure a parallel arrangement between the oxazole rings is realized indicating π - π stacking of them with a distance between them of around 3.545 and 3.638 Å (Fig. 4).

Complex **3** crystallizes in the triclinic space group *P*1, and its ORTEP structure along with the atomic numbering scheme is

shown in Fig. 5. The asymmetric unit of **3** contains one Ag atom, two 4-PBO ligands and one picrate anion. As illustrated in Fig. 5, the Ag(I) ion is four-coordinated (N2 and N4 atoms from two 4-PBO ligands, two oxygen atoms from picrate anions) with a seesaw conformation ($\tau = 0.44$). The parameter τ is defined as $[360-(\alpha + \beta)]/141$ [where $\beta = N(2)-Ag(1)-N(4)$, $\alpha = O(4)-Ag(1)-O(9)$] and its value varies from 0 (in regular square planar geometry) to 1 (tetrahedral) [37]. The picrate anion ligand bridges Ag atoms with a one-dimensional linear polymer and the aromatic rings of the 4-PBO ligands paralleling each other. Furthermore, there are two kinds of face-to-face π - π stacking in **3**. One is between pyridine rings of adjacent layers with the centroid–centroid distance of 3.6187(3) Å and interplanar separation being 3.331(3) Å, and the other is between oxazole and benzene rings of benzoxazole of

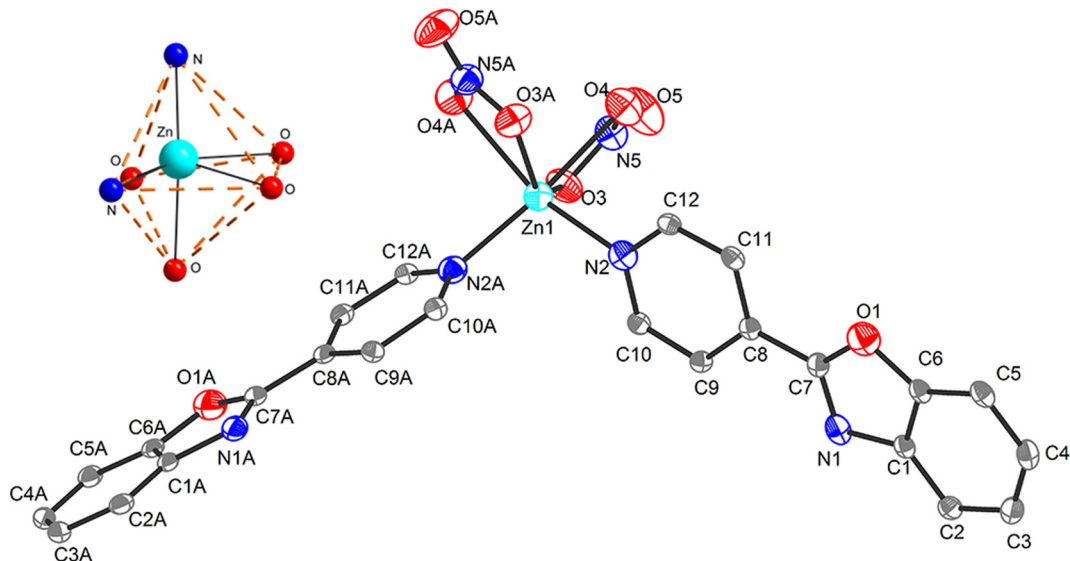


Fig. 3. Molecular structure and atom numberings of complex **2** showing displacement ellipsoids at the 30% probability level. Hydrogen atoms were omitted for clarity.

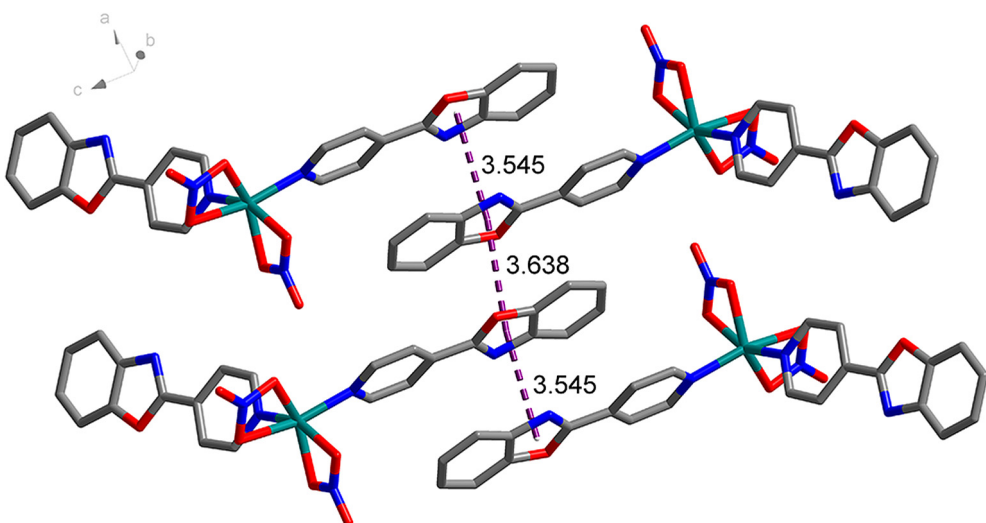


Fig. 4. 2D supramolecular layer of **2** viewed along the [101] plane, showing the π - π stacking interactions as purple broken lines. (Color online.)

the 4-PBO ligands with the centroid–centroid length of 3.7587(3) Å and interplanar separation of 3.516(3) Å, yielding a 3D supramolecular framework through the two types of strong π - π interactions.

A close look into the structures of complexes **1** and **2** reveals that the metal centers play key roles on the frameworks of the complexes. Since Zn(II) and Cd(II) are d¹⁰ systems that do not possess crystal field stabilization energy and the effect of steric repulsion between different ligands (3-PBO, 4-PBO) might be slight, the coordination numbers of Zn(II) and Cd(II) ions are mainly determined by the radius of central metal ion. The Cd(II) ion radius is larger than that of Zn(II) ion, therefore the coordination numbers of Cd(II) ion in **1** are 7 and Zn(II) ion in **2** are 6.

3.2. IR and UV spectra

The IR spectral data for the free ligands and three metal complexes with their relative assignments have been studied to characterize their structures. The IR spectra of 4-PBO are closely

related to those of the free ligand 3-PBO. The spectrum of 3-PBO shows a strong band at 1454 cm⁻¹, which is assigned to v(C=N) [38]. In comparison with the IR spectra of the ligands, all the metal complexes exhibit blue shift 41–59 cm⁻¹ of v(C=N) indicating the participation of imine nitrogen atoms in the coordination to the metal ion. Moreover, complexes **1** and **2** appear two new bands at 1300, 1041 cm⁻¹ and 1346, 1032 cm⁻¹ respectively, which indicate that nitrate are coordinated to the metal ions center [38]. This deduction agrees with the results of the X-ray crystal structure determinations.

The electronic spectra of the ligands and metal complexes were recorded in DMF solution at room temperature. The UV band of 3-PBO (301 nm) is only marginally red-shifted about 2 nm for complex **1**, which is evidence of C=N (pyridine) coordination to the metal center. Analogously, the UV bands of 4-PBO (300 nm) are red-shifted about 2–3 nm in complex **2** and complex **3** respectively. This phenomenon also shows that C=N is involved in coordination to the metal center. The picrate bands of complex **3** (observed at 380 nm) are assigned to $\pi \rightarrow \pi^*$ transitions [39].

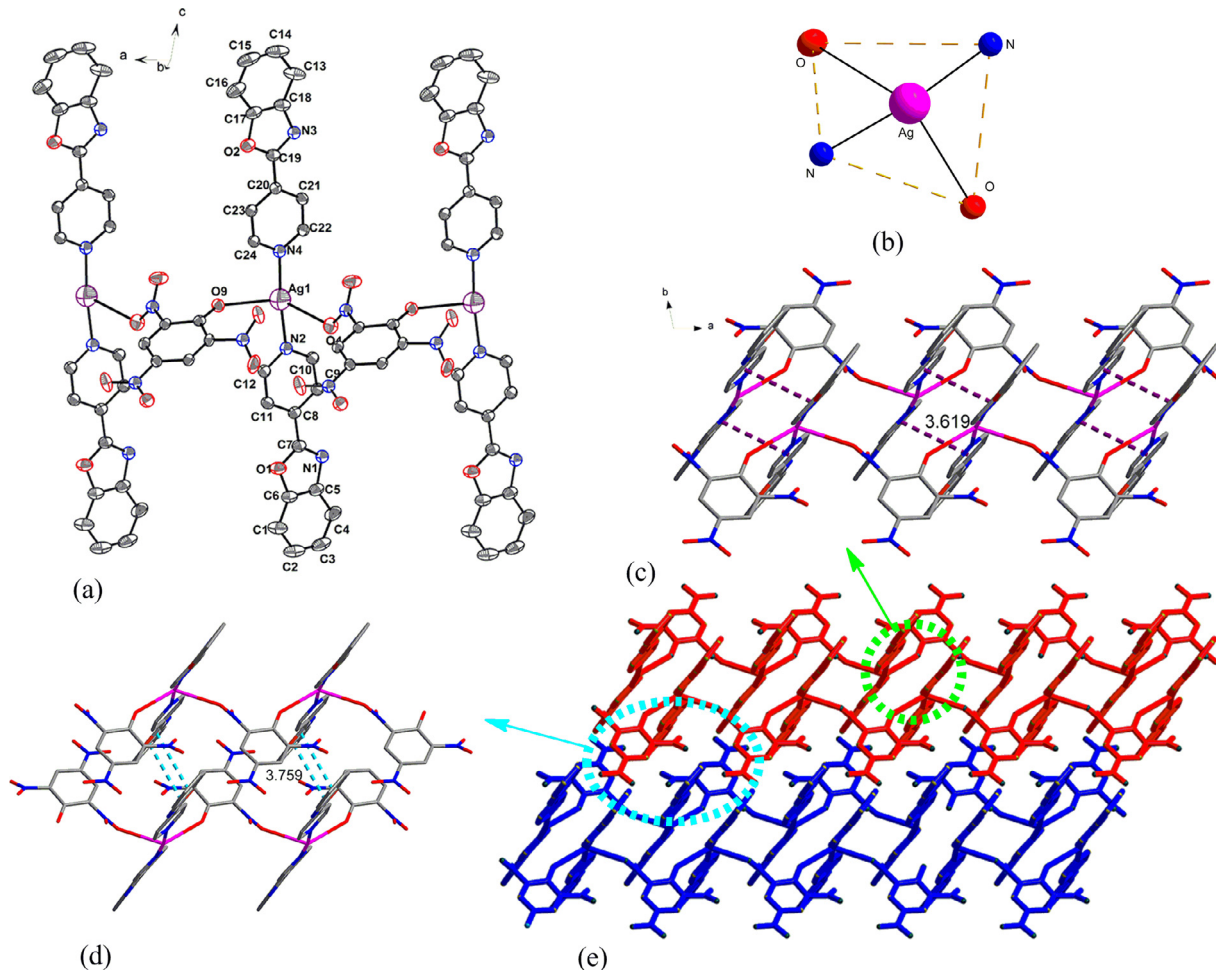


Fig. 5. (a), (b) Molecular structure and atom numberings of complex **3** showing displacement ellipsoids at the 30% probability level. (Hydrogen atoms were omitted for clarity), (c), (d) 2D supramolecular layer of **3** viewed along in the *ab* plane, showing the π - π stacking interactions. (d) The 3D supramolecular network formed by two types (green and blue) of π - π stacking interactions of **3**. (Color online.)

3.3. Thermal analyses of complexes **1–3**

To study the stabilities of the three complexes, the thermogravimetric analysis under nitrogen atmosphere was performed with a heating rate of 10 °C/min. As shown in Fig. 6, the complex **1** revealed obvious two-step mass-loss process. Firstly, the weight loss of 10.3% in the range 87–210 °C corresponds to the release of the two lattice water and acetonitrile molecules (calcd 10.8%). The successive mass loss at the temperature range of 210 to above 800 °C may be attributed to the gradual removal of ligand, nitrate radicals and the rest of CdO. Complex **2** displayed a first weight loss region from 108 to 210 °C, assigned to release of the nitrate radicals of crystallization molecules (obsd 10.9%, calcd 10.7%). Then, there was formation of a plateau region observed from 210 to 252 °C. The subsequent mass loss at the temperature range of 252 to above 800 °C is explained on the basis of the stepwise removal of ligand and the remainder of ZnO. Complex **3** could resist decomposition until to 211 °C, and then undergoes a large loss-weight process from 211 to 403 °C with a weight-loss of 72% corresponding to the release of all ligands (calculated value 71%). The successive mass loss from 403 to above 800 °C may be the result of the gradual removal of ligand and the remainder of AgO.

3.4. Luminescent properties of the free ligands and their complexes

Luminescent compounds are of great current interest because of their various applications in chemical sensors, photochemistry, and electroluminescent display [40].

The fluorescent emission spectra of the ligands (3-PBO and 4-PBO) and their three complexes **1–3** were measured in a solid state at room temperature as shown in Fig. 7(a), (b). Fig. 7(c) depicts the colour and luminescence changes for these compounds under ambient light and UV light irradiation (365 nm). The free ligands 3-PBO and 4-PBO show purple fluorescent luminescence with the maximum wavelengths at 392 nm and 406 nm when excited at 340 nm and 358 nm, respectively, significantly assigned to π - π^* transition fluorescence. When complex **1** is excited at 340 nm, a strong emission band is observed at 404 nm, which is red shifted in comparison to its related ligand 3-PBO. In addition, complexes **2** exhibits intense fluorescent emission bands at 429 nm upon excitation at 358 nm, which is also red shifted in comparison to its related ligand 4-PBO. To our knowledge, because Zn(II) and Cd (II) are d^{10} systems, it is really difficult for these to undergo oxidation or reduction process. The spectral behavior of these complexes is neither due to metal-to-ligand nor ligand-to-metal charge transfer transition. Hence, metal perturbed intraligand π - π^* charge

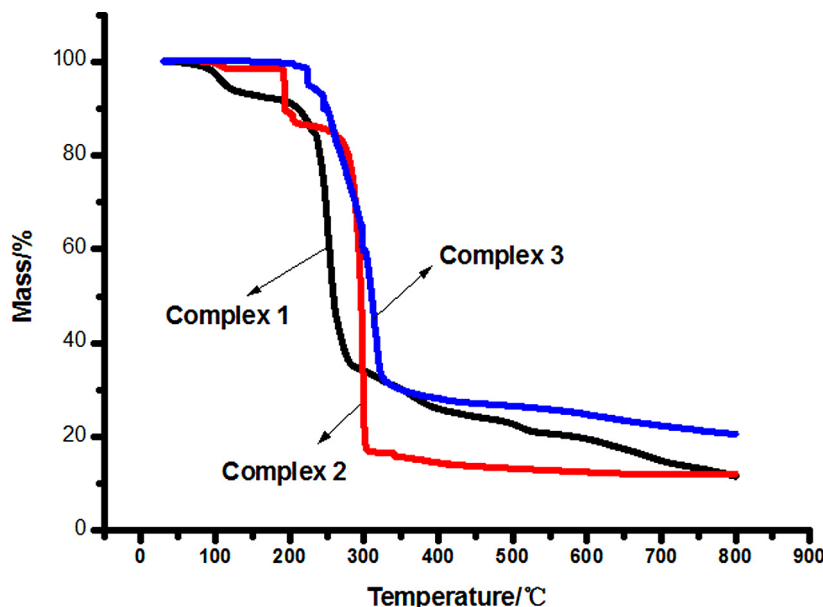


Fig. 6. TG curves of complexes 1–3.

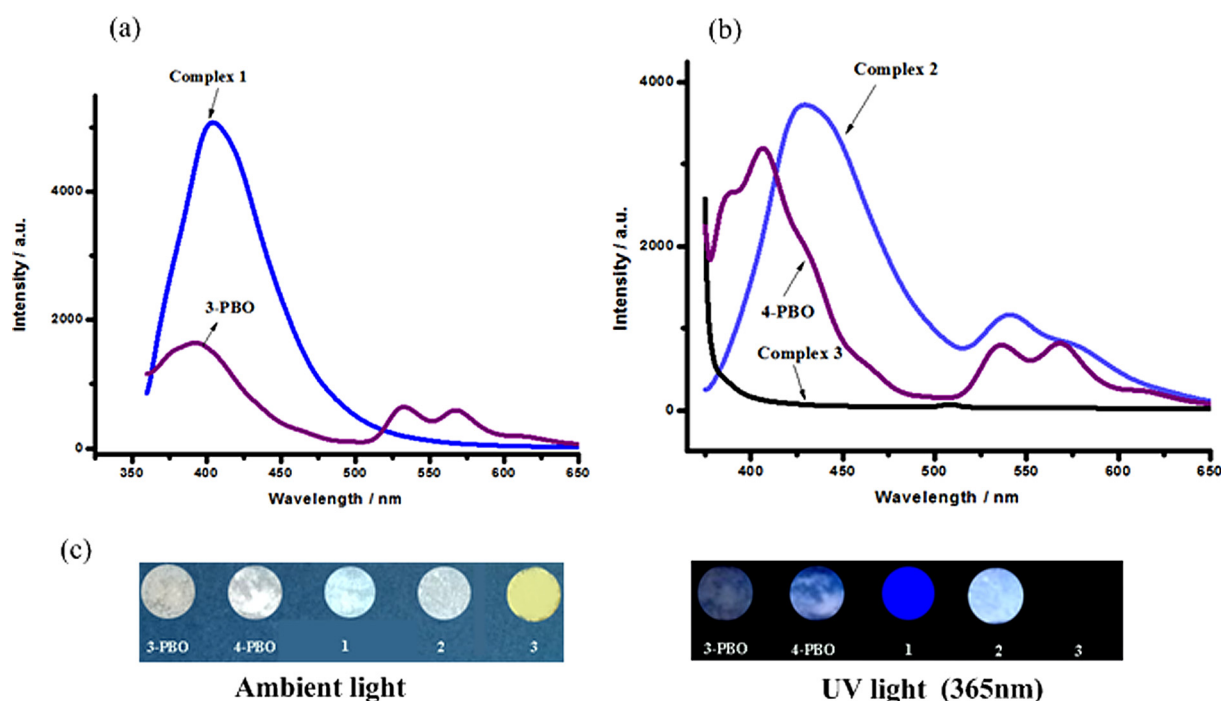


Fig. 7. (a), (b) The solid-state fluorescent emission spectra of the ligands and the complexes. (c) Photographic images of ligands and the complexes under ambient light and UV light irradiation (365 nm).

Table 4
Electrochemical data of complex 3.

Complex	E_{pc}	E_{pa}	ΔE_p	$E_{1/2}$	i_{pa}	i_{pc}	I
3	0.373	0.621	0.248	0.497	57.498	-17.835	3.224

$\Delta E = E_{pa} - E_{pc}$; $E_{1/2} = (E_{pa} + E_{pc})/2$; $I = i_{pa}/i_{pc}$.

transfer transition is responsible for the emission behavior of the reported complexes [41]. Moreover the enhancement and shift of the emissions for complexes **1** and **2** compared to 3-PBO and 4-PBO may be attributed to the fact that the coordination of metal ions increases the ligand conformational rigidity and reduces the loss of energy by radiationless decay of the intraligand emission excited state [42]. During complexation, quenching of fluorescence of complexes **3** is a somewhat common phenomenon, which is

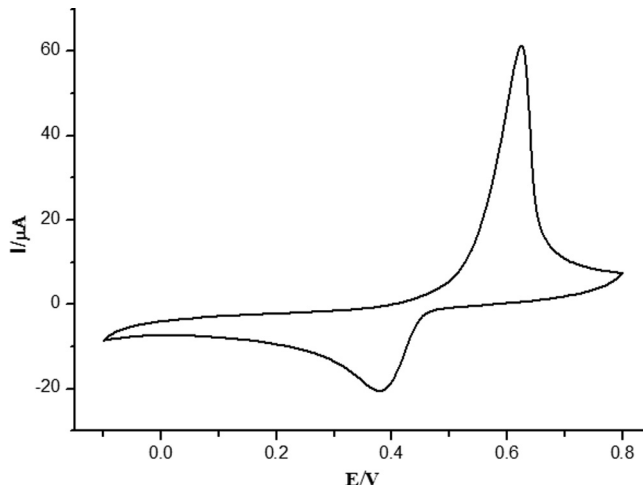


Fig. 8. Cyclic voltammogram of **3** recorded with a platinum electrode in DMF solution containing $(\text{nBu})_4\text{N-ClO}_4$ (0.1 M) (scan rate = 0.10 V-S^{-1}).

attributed to processes such as magnetic perturbation, redox activity, unpaired electrons, heavy-atom effects and electronic energy transfer [43].

3.5. Electrochemical studies

The electrochemical properties of **3** were studied by cyclic voltammetry (CV) in DMF. The data are collected in Table 4 and a voltammogram is shown in Fig. 8. The Ag(I) complex exhibits a pair of cathodic and anodic waves. The separation between the cathodic and anodic peak potentials ΔE_{p} ($E_{\text{pa}} - E_{\text{pc}}$) and the current I ($i_{\text{pa}}/i_{\text{pc}}$) indicate a quasi-reversible redox process assignable to the Ag(I)/Ag couple. The free 4-PBO ligand is not electroactive over the range -0.2 to $+0.8$ V. According to previous reports [44], a transition metal complex must have a redox potential below 0.65 V [$E^{\circ}(\text{O}_2-\text{O}_2^-)$] and above -0.33 V [$E^{\circ}(\text{O}_2-\text{O}_2^-)$] such that catalysis can be an effective mimic of superoxide dismutase but toxic single oxygen cannot be formed; so the redox potential 0.248 V shows that **3** may have SOD activity.

4. Conclusion

In conclusion, the successful of aromatic ligands 3-PBO and 4-PBO with their complexes have been synthesized and characterized. The single crystal X-ray diffraction analysis shows the complexes **1–3** lead to three novel two- or three-dimensional supramolecular structures, respectively. Experimental results indicated that complex **1** showed strong luminescence than any other compounds in solid-state. All of them present good thermal stability. Moreover, Electrochemical studies show quasi-reversible redox behavior for the complex **3**. These findings indicate that the transition metal complexes have many potential practical applications for the development of luminescence and electrochemistry.

Acknowledgements

The present research was supported by the National Natural Science Foundation of China (Grant No. 21367017), Foundation of A Hundred Youth Talents Training Program of Lanzhou Jiaotong University and Natural Science Foundation of Gansu Province (Grant No. 1212RJZA037).

Appendix A. Supplementary material

CCDC 1519464, 1519465 and 1519466 contains the supplementary crystallographic data for complexes **1–3**. These data can be obtained free of charge via <http://www.ccdc.cam.ac.uk/conts/retrieving.html>, or from the Cambridge Crystallographic Data Centre, 12 Union Road, Cambridge CB2 1EZ, UK; fax: (+44) 1223-336-033; or e-mail: deposit@ccdc.cam.ac.uk.

References

- [1] S. Miyazaki, T. Kojima, S. Fukuzumi, *J. Am. Chem. Soc.* **130** (2008) 1556.
- [2] M. Dinca, A.F. Yu, J.R. Long, *J. Am. Chem. Soc.* **128** (2006) 17153.
- [3] J.R. Li, Q. Yu, Y. Tao, X.H. Bu, J. Ribas, S.R. Batten, *Chem. Commun.* **48** (2007) 2290.
- [4] W.X. Chai, L. Song, J. Li, K.Y. Shu, L.S. Qin, H.S. Shi, J.Y. Guo, *J. Inorg. Organomet. Polym.* **22** (2012) 1263.
- [5] (a) L.M. Chiang, C.W. Yeh, Z.K. Chan, K.M. Wang, Y.C. Chou, J.D. Chen, J.C. Wang, J.Y. Lai, *Cryst. Growth Des.* **8** (2008) 470;
(b) H.C. Chen, H.L. Hu, Z.K. Chan, C.W. Yeh, H.W. Jia, C.P. Wu, J.D. Chen, J.C. Wang, *Cryst. Growth Des.* **7** (2007) 698;
(c) T.L. Hu, R.Q. Zou, J.R. Li, X.H. Bu, *Dalton Trans.* **10** (2008) 1302;
(d) D. Sun, N. Zhang, R.B. Huang, L.S. Zheng, *Cryst. Growth Des.* **10** (2010) 3699.
- [6] M. Yoshizawa, M. Tamura, M. Fujita, *Science* **312** (2006) 251.
- [7] I.A. Gural'skiy, D. Escudero, A. Frontera, P.V. Solntsev, E.B. Rusanov, A.N. Chernega, H. Krautscheid, K.V. Domasevitch, *Dalton Trans.* **15** (2009) 2856–2864.
- [8] R.R. Tidwell, S.K. Jones, N.A. Naiman, L.C. Berger, W.B. Brake, C.C. Dykstra, J.E. Hall, *Antimicrob. Agents Chemother.* **37** (1993) 1713.
- [9] L.H. Gao, M. Guan, K.Z. Wang, L.P. Jin, C.H. Huang, *Eur. J. Inorg. Chem.* **2006** (2006) 3731.
- [10] Y.P. Tong, S.L. Zheng, X.M. Chen, *Inorg. Chem.* **44** (2005) 4270.
- [11] D. Moon, M.S. Lah, R.E.D. Sesto, J.S. Miller, *Inorg. Chem.* **41** (2002) 4708.
- [12] A. Barbieri, G. Accorsi, N. Armarelli, *Chem. Commun.* **2008** (2008) 2185.
- [13] R.C. Evans, P. Douglas, C. Winscom, *J. Coord. Chem. Rev.* **250** (2006) 2093.
- [14] P. Ovejero, E. Asensio, J.V. Heras, J.A. Campo, M. Cano, M.R. Torres, C. Núñez, C. Lodeiro, *Dalton Trans.* **42** (2013) 2107.
- [15] (a) T. Sano, Y. Nishio, Y. Hamada, H. Takahashi, T. Usuki, K. Shibata, *J. Mater. Chem.* **10** (2000) 157;
(b) S. Tokito, K. Noda, H. Tanaka, Y. Taga, T. Tsutsui, *Synth. Met.* **111–112** (2000) 393.
- [16] I.P. Oliveri, S. Di Bella, *Tetrahedron* **67** (2011) 9446.
- [17] (a) M.E. Germain, M.J. Knapp, *J. Am. Chem. Soc.* **130** (2008) 5422;
(b) M.E. Germain, T.R. Vargo, P.G. Khalifah, M.J. Knapp, *Inorg. Chem.* **46** (2007) 4422.
- [18] Y.Q. Gong, J. Fan, R.H. Wang, Y.F. Zhou, D.Q. Yuan, M.C. Hong, *J. Mol. Struct.* **705** (2004) 29.
- [19] W. Li, O.R. Evans, R.G. Xiong, Z. Wang, *J. Am. Chem. Soc.* **120** (1998) 13272.
- [20] W.B. Lin, Z.Y. Wang, L. Ma, *J. Am. Chem. Soc.* **121** (1999) 11249.
- [21] Y.B. Chen, J. Zhang, J.K. Cheng, Y. Kang, Z.J. Li, Y.G. Yao, *Inorg. Chem. Commun.* **7** (2004) 1139.
- [22] J.L. Barriada, A.D. Tappin, E.H. Evans, E.P. Achterberg, *Trends Anal. Chem.* **26** (2007) 809.
- [23] H.T. Ratte, *Environ. Toxicol. Chem.* **18** (1999) 89.
- [24] Y. Zhou, W. Chen, D. Wang, *Dalton Trans.* **11** (2008) 1444.
- [25] (a) H.L. Wu, F. Kou, F. Jia, B. Liu, J.K. Yuan, Y. Bai, *J. Coord. Chem.* **64** (2011) 3041;
(b) H.L. Wu, J.K. Yuan, Y. Bai, H. Wang, G.L. Pan, J. Kong, *J. Photochem. Photobiol. B* **116** (2012) 13;
(c) H.L. Wu, X.C. Huang, J.K. Yuan, F. Kou, F. Jia, B. Liu, K.T. Wang, *Eur. J. Med. Chem.* **45** (2010) 5324;
(d) H.L. Wu, H.P. Peng, Y.H. Zhang, F. Wang, H. Zhang, C.P. Wang, Z.H. Yang, *Appl. Organometal. Chem.* **29** (2015) 443;
(e) H.L. Wu, F. Wang, F.R. Shi, Z.H. Yang, H. Zhang, H.P. Peng, *Transition Met. Chem.* **40** (2015) 555;
(f) H.L. Wu, H. Zhang, F. Wang, H.P. Peng, Y.M. Cui, Y.Y. Li, Y.H. Zhang, *J. Chem. Res.* **39** (2015) 76.
- [26] M.S. Park, K. Jun, S.R. Shin, S.W. Oh, *J. Heterocyclic Chem.* **39** (2002) 1279.
- [27] Bruker, SMART, SAINT AND SADABS, Bruker Axs, Inc., Madison, Wisconsin, USA, 2000.
- [28] G.M. Sheldrick, *SHELXTL*, Siemens Analytical X-Ray Instruments Inc., Madison, Wisconsin, USA, 1996.
- [29] C.W. Chan, C.M. Che, *Polyhedron* **12** (1993) 2169.
- [30] F. Guo, J. Xu, X. Zhang, B. Zhu, *Inorg. Chim. Acta* **363** (2010) 3790.
- [31] R.H. Wang, L. Han, P.L. Jing, Y.F. Zhou, D.Q. Yuan, M.C. Hong, *Cryst. Growth Des.* **5** (2005) 129.
- [32] (a) H.L. Wu, K.T. Wang, F. Jia, B. Liu, F. Kou, J.K. Yuan, J. Kong, *J. Coord. Chem.* **63** (2010) 4113;
(b) H.L. Wu, K.T. Wang, F. Kou, F. Jia, B. Liu, J.K. Yuan, Y. Bai, *J. Coord. Chem.* **64** (2011) 2676.
- [33] L.E. Xiao, M. Zhang, W.H. Sun, *Polyhedron* **29** (2010) 142.
- [34] D. Kang, J. Seo, S.Y. Lee, J.Y. Lee, *Inorg. Chem. Commun.* **10** (2007) 1425.

- [35] N. Yoshikawa, S. Yamabe, N. Kanehisa, Y. Kai, H. Takashima, K. Tsukahara, *Eur. J. Inorg. Chem.* 13 (2007) 1911.
- [36] J.P. Collin, I.M. Dixon, J.P. Sauvage, J.A.G. Williams, F. Barigelletti, L. Flamigni, *J. Am. Chem. Soc.* 121 (1999) 5009.
- [37] L. Yang, D.R. Powell, R.P. Houser, *Dalton Trans.* 9 (2007) 955.
- [38] (a) H.L. Wu, Y.C. Bai, Y.H. Zhang, *J. Coord. Chem.* 67 (2014) 3054;
(b) G.L. Pan, Y.C. Bai, H.W.J. Kong, F.R. Shi, Y.H. Zhang, X.L. Wang, H.L. Wu, *Z. Naturforsch.* 68b (2013) 257–266;
(c) H.L. Wu, F. Jia, F. Kou, B. Liu, J.K. Yuan, Y. Bai, *Transition. Met. Chem.* 36 (2011) 847;
(d) K. Nakamoto, *Infrared and Raman Spectra of Inorganic and Coordination Compounds*, 4th ed., John Wiley & Sons, New York, 1986, p. 284.
- [39] H.L. Wu, K. Li, T. Sun, F. Kou, F. Jia, J.K. Yuan, B. Liu, B.L. Qi, *Transition. Met. Chem.* 36 (2011) 21.
- [40] (a) Q. Wu, M. Esteghamatian, N.X. Hu, Z. Popovic, G. Enright, Y. Tao, M. D'Iorio, S. Wang, *Chem. Mater.* 12 (2000) 79;
(b) J.E. McGarrah, Y.J. Kim, M. Hissler, R. Eisenberg, *Inorg. Chem.* 40 (2001) 4510;
- (c) G.D. Santis, L. Fabbrizzi, M. Licchelli, A. Poggi, A. Taglietti, *Angew. Chem., Int. Ed. Engl.* 35 (1996) 202.
- [41] M. Bera, S.K. Jana, A. Rana, D.S. Chowdhuri, D. Hazari, C.M. Liu, E. Zangrandi, S. Dalai, *J. Inorg. Organomet. Polym.* 23 (2013) 736.
- [42] (a) Q. Chu, G.X. Liu, T. Okamura, Y.Q. Huang, W.Y. Sun, N. Ueyama, *Polyhedron* 27 (2008) 812;
(b) H. Yersin, A. Vogler (Eds.), *Photochemistry and Photophysics of Coordination Compounds I*, Springer, Berlin, 1987;
(c) A. Vogler, H. Kunkely, *Coord. Chem. Rev.* 250 (2006) 1622;
(d) L. Wen, Y. Li, Z. Lu, J. Lin, C. Duan, Q. Meng, *Cryst. Growth. Des.* 6 (2006) 530.
- [43] (a) Q. Ye, X.B. Chen, Y.M. Song, X.S. Wang, J. Zhang, R.G. Xiong, H.K. Fun, X.Z. You, *Inorg. Chim. Acta* 358 (2005) 1258;
(b) G.B. Bagihalli, P.G. Avaji, S.A. Patil, P.S. Badami, *Eur. J. Med. Chem.* 43 (2008) 2639;
(c) J. Chan, S.C. Dodani, C.J. Chang, *Nat. Chem.* 4 (2012) 973.
- [44] H.L. Wu, R.R. Yun, K.T. Wang, K. Li, X.C. Huang, T. Sun, Y.Y. Wang, Z. Anorg. Allg. Chem. 636 (2010) 1397.